Continuous Fractionation and Solution Properties of PIB. I. Search for the Best Mixed Solvent and First Results of the Continuous Polymer Fractionation

H. GEERISSEN, J. ROOS, P. SCHUTZEICHEL and B. A. WOLF,
Institut für Physikalische Chemie der Universität Mainz, Jakob-Welder-Weg 15, D-6500 Mainz, West Germany

Synopsis

To adopt a recently developed method for large scale fractionation (CPF = continuous polymer fractionation, a special kind of counter current extraction) to polyisobutylene (PIB), a systematic search for the best mixed solvent was performed. For this purpose, the essential parts of the phase diagrams solvent/nonsolvent/PIB were determined for 21 mixed solvents by cloud-point measurements; with eight systems of special interest, the molecular weight distributions of the polymers contained in the coexisting phases were also studied. On the basis of these experiments and of considerations concerning additional criteria for the performance of the continuous counter current extraction, the mixed solvent toluene/methyl ethyl ketone was chosen. First experiments with a PIB sample of M_w = 420,000 g/mol and a molecular nonuniformity $U = (M_w/M_n) - 1$ of 2.3 yielded two high molecular weight fractions ($M_w = 1.1 \times 10^6$ and 0.6×10^6 resp.), with $U = 0.3$ on a 100 g scale upon the application of four CPF steps.

INTRODUCTION

In contrast to the classical continuous countercurrent extraction, the recently developed CPF[1,2] does not make use of a miscibility gap between two low molecular weight liquids, but functions on the basis of the limited solubility of the polymer in a mixed thetasolvent (1 = solvent, 2 = nonsolvent) or in a single theta solvent. A comparatively concentrated solution of the polymolecular polymer* is extracted continuously by an extracting agent (EA), which is normally the pure solvent, using a sieve bottom column with pulsator. By means of a proper selection of the operating conditions (like flow ratio $\dot{q} = \dot{V}^{EA}/\dot{V}^{FD}$ as well as frequency and amplitude of pulsation), the molecular weight distribution of the original polymer can be cut into two pieces at the desired position such that practically all shorter chains are extracted by the solvent which leaves the column as the sol (SL) and all longer ones remain in the feed phase yielding the gel (GL). The weight ratio of the polymer transported in these phases per unit time, $\dot{m}_3^{SL}/\dot{m}_3^{GL}$ (3 = polymer), is called $\dot{G}$.

The present part of this series on PIB describes the preparatory work, necessary for a successful application of the CPF, i.e., the search for the most apt mixed solvents, and first results with that method. A broader discussion of

*Feed = FD.

Journal of Applied Polymer Science, Vol. 34, 271–285 (1987)
 CCC 0021-8995/87/010271-15$04.00

TABLE I
List of Solvents

Solvent	Abbrev	Producer/purity	Density (g cm^{-1})
Toluene	TOL	Merck, p.a. ≥ 99%	0.867
Cyclohexane	CH	Merck-Schuchardt, for synthesis, ≥ 99%	0.778
n-Heptane	HEP	Fluka, pure, ≥ 99%	0.684
n-Dibutylether	DBE	Merck-Schuchardt, for synthesis, ≥ 99%	0.768
Siedegrenzen-Benzin 2 (petrol fraction 100–130°C)	BENZ 2	Fluka, pure	0.72
Siedegrenzen-Benzin 3 (petrol fraction 110–140°C)	BENZ 3	Fluka, pure	0.73
Tetrahydrofuran	THF	Merck, p.a. ≥ 99.5%	0.887
2-Butanone	MEK	Merck, p.a. ≥ 99.5%	0.804
Acetone	AC	Merck, p.a. ≥ 99.5%	0.790
2-Propanol	JPA	Merck, for spectroscopy, ≥ 99.7%	0.783

how the CPF functions is given in Part II, which deals with the optimization of the CPF, i.e., studies the effects of changes in the operating conditions on the fractionation efficiency. The next two parts describe the physicochemical behavior of the PIB fractions obtained from the CPF in dilute (Part III) and in moderately concentrated solutions (Part IV).

EXPERIMENTAL

Materials

The PIB sample used for the present study was Oppanol B 50 (BASF, Ludwigshafen); its M_w value is 420,000 and its nonuniformity $U \approx 2.3$ ($U = (M_w/M_n) - 1$). In the following, this starting material is abbreviated PIB I. Table I contains the solvents, their producer, purity grade, and densities.

Procedure

Cloud Point Titration. The limits of complete miscibility were determined ($T = 22$°C) visually by means of adding the nonsolvent to solutions of PIB I in the pure solvent up to the point, at which the scale on the back side of a glass tube could no longer be read.

Coexisting Phases. The solutions were prepared in special glass tubes with KF screwing (Fa. Kühn, Hagen, West Germany) by adding the nonsolvent to the polymer dissolved in the pure solvent. This mixture was homogenized by stirring and heating above the cloud-point temperature and then thermostatted at the equilibrium temperature of 22°C until complete phase separation was achieved. The coexisting phases were separated by means of a syringe, and the solvent components were evaporated under high vacuum and collected in a condenser. The polymer content was determined gravimetrically and the composition of the mixed solvent in the coexisting phases by refractometry.

CPF. Central component of the CPF apparatus is a commercially available sieve bottom column with pulsator (Fa. Quickfit, Wiesbaden, West Germany), which is suitable for the fractionation of a maximum of 1 g polymer/min. For details, see Part II.

Drying of PIB. The polymer was dried by pumping off all volatile components (at max. 40°C), redisolving the remainder in CH and repeating this procedure. Finally the polymer was freeze-dried from solutions in CH.

Light Scattering (LS). LS measurements were performed on the commercially available instrument Fica 50 (Fa. Sofica, France) with vertically polarized light (546 nm) in isooctane (Merck p.a., ≥ 99.5%) as solvent. The value of the refractive index increment, dn/dc, is equal to 0.139 cm^3/g at 25°C.[3]

GPC. The system consists of μ-Styragel columns with 10^4, 10^5, and two 10^6 Å pore diameter. THF was used as eluent, and the volume of the injected polymer solution (2×10^{-3}g polymer/cm^3) was 50μL. The composition of the effluent stream is detected by means of a differential refractometer from Showadenko. The column set was calibrated with ca. 25 fractionated PIB samples, products from the CPF, and of discontinuously performed fractionations (cf. Part III), which had been characterized by LS. The resulting log M vs. V_e plot is shown in Figure 1. A possible broading of the elution peak due to axial dispersion was taken into account by subtracting an excess nonuniformity U_{ex} according to[4]

$$U = (1 + U_{app})/(1 + U_{ex}) \approx U_{app} - U_{ex}$$

U_{ex} was determined from very narrowly distributed PS samples (Fa. Knaur,

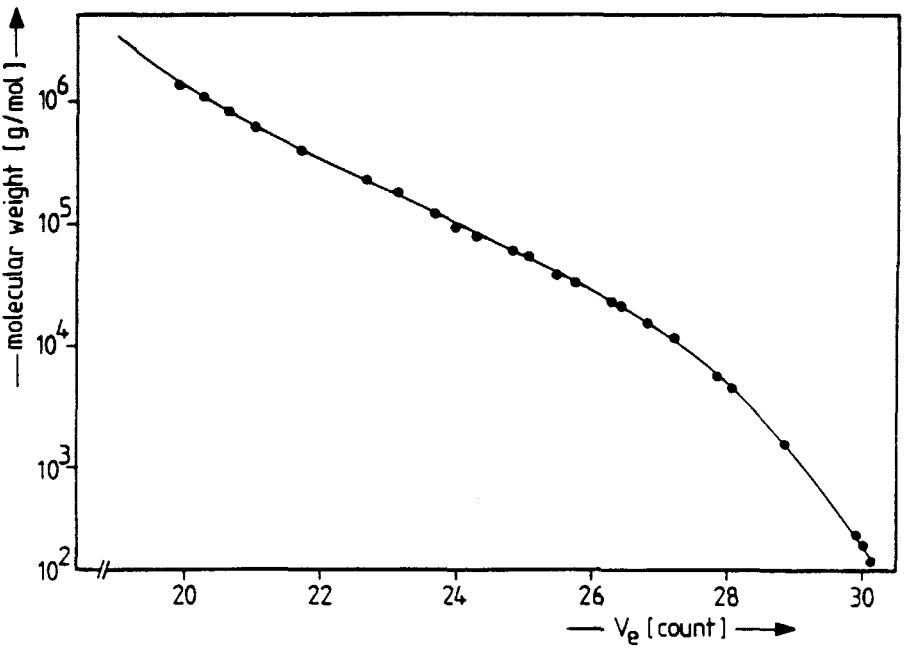

Fig. 1. GPC-calibration curve for PIB in THF at 25°C.

Berlin, West Germany, $M_w = 233{,}000$ and $U = 0.01$ determined by phase distribution chromatography[5]) to be 0.05 ± 0.01.

RESULTS AND DISCUSSION

Scruting of Mixed Solvents

The most important prerequisite for a successful application of the CPF is a suitable solvent/nonsolvent system. Like all other fractionation methods resting upon a "fractionation by solubility," a pair of thermodynamically similar components is generally preferred (cf. Baker–Williams fractionation[6]). However, in the case of the CPF, other criteria like the kinetics of the phase separation, operating temperature of the system, and, last but not least, the availability of large amounts of solvents have to be considered.

Phase Diagrams. In order to obtain initial information concerning the location of the miscibility gaps of the different solvent/nonsolvent systems, cloud-point determinations were made in a concentration range between 2 and 7 wt % of PIB. For this purpose each of the solvents of Table I was combined with the three nonsolvents AC, MEK, and IPA. The sections of the phase diagrams shown in Figure 2 reveal that the influence of the solvent component on the position of the miscibility gap increases in the order IPA, AC, MEK.

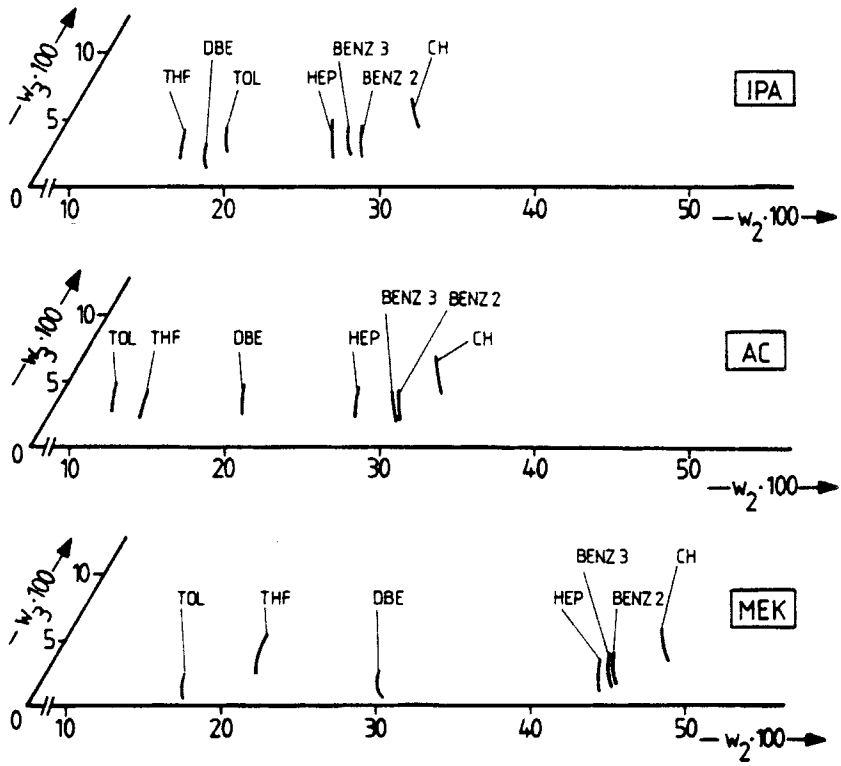

Fig. 2. Scrutiny of the phase separation behavior of PIB I (index 3) with the different combinations of solvents (index 1) and nonsolvents (index 2) at 22°C; in each of the three phase diagrams (w = weight fraction) shown in part, the nonsolvent component (boxed in on the right-hand side of these graphs) is combined with the different solvents indicated at the cloud point curves; for abbreviations, cf. Table I.

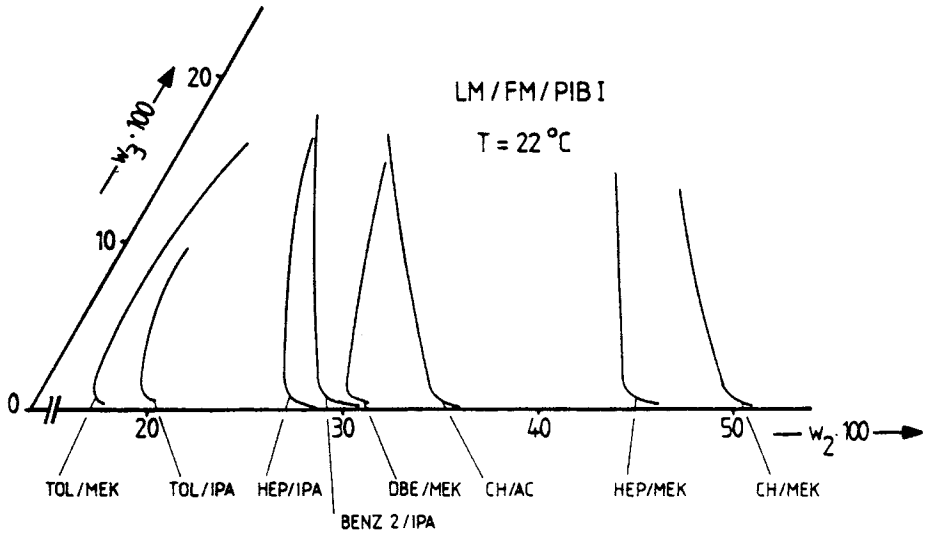

Fig. 3. Cloud point curves of PIB I dissolved in the indicated mixed solvents (for abbreviation cf. Table I); w_2, w_3 = weight fractions of nonsolvent and of polymer.

With all three nonsolvents the amount of solvent required to achieve homogenous conditions for a given polymer concentration increases in the order CH, BENZ 2, BENZ 3, HEP, DBE, THF; only TOL derivates from a common sequence: In combination with AC and MEK it constitutes the worst solvent, whereas it falls between MEK and DBE in the case of IPA. To gain more information on the most promising systems, larger portions of their solubility gaps were determined. Figure 3 shows the results of these measurements.

Coexisting Phases. In order to estimate the fractionation effect in the different mixed solvents, the ratio of the total mass of polymer in the sol phase to that in the gel phase, i.e., the value $G = m_3^{SL}/m_3^{GL}$ (analogous to G) was determined, as well as the molecular weight distribution of the polymer contained in the coexisting phases (cf. Fig. 4). To simplify the evaluation, only the maxima of the GPC elution peaks (M_{GPC}) and their halfwidth ($b_{1/2}$) were compared. In addition, the composition of the mixed solvent contained in the coexisting phases was also determined. In order to stay within the normal operating range of the CPF, w_3 was chosen as 0.03 and $\Delta w_2 = 0.01, 0.05$, and 0.09 ($\Delta w_2 = w_2 - w_{2,cp}$, where $w_{2,cp}$ is the weight fraction of the nonsolvent at the cloud point). All results are compiled in Table II. Instead of the detailed data concerning the preferential incorporation of the components of the mixed solvents into the coexisting phases, only the type[7] of the mixed solvent is given. Systems showing an enrichment of the solvent component in the gel phase are therein called type I; for type II, on the other hand, the solvent component is preferentially incorporated into the sol phase. DBE/MEK/PIB I is the only system that is not entirely of type I since it changes from type I to type II as the mixed solvent becomes richer in nonsolvent.

Search for the Best Mixed Solvent

Fractionation Efficiency. The most important question is: What fractionation is associated with a certain subdivision of the starting material according to weight into two fractions (measured by G) at constant polymer

TABLE II
Analysis of the Phases Coexisting at 22°C

Mixed solvent	Composition[a]	Cloud point temp (°C)	Mixed solvent type (cf. text)	G	M_{GPC} (g mol^{-1}) gel/sol	$b_{1/2}$ (cm) gel/sol
TOL/MEK	1	23.1	I	0.65	707,000/255,400	2.75/4.40
	2	32.5		0.08	536,100/48,300	3.65/3.20
	3	41.0		0.05	519,900/29,100	4.00/2.80
TOL/JPA	1	26.5	I	0.44	595,300/158,300	3.00/4.50
	2	40.5		0.12	530,000/48,000	3.90/3.10
	3	57.0		0.04	501,100/48,000	3.80/3.15
HEP/MEK	1	26.6	I	0.61	633,800/208,600	2.80/3.90
	2	46.0		0.13	540,000/48,300	3.70/3.10
	3	69.0		0.05	490,000/26,800	4.35/2.78
HEP/IPA	1	31.3	I	0.49	563,100/172,500	2.95/3.70
	2	64.0		0.11	523,100/43,200	3.80/3.15
	3	93.8		0.03	498,000/24,000	4.10/2.65
CH/MEK	1	27.0	I	0.38	570,100/155,400	3.10/3.90
	2	44.0		0.09	505,500/34,900	4.20/3.00
	3	62.5		0.05	486,000/20,600	4.35/2.55
CH/AC	1	25.2	I	0.36	552,800/165,200	3.10/4.00
	2	45.3		0.04	510,000/34,700	3.95/3.10
	3	68.0		0.01	491,700/17,000	4.00/2.40
DBE/MEK	1	25.9	I	0.80	702,500/244,600	2.75/4.00
	2	42.5	II	0.13	520,000/64,300	3.50/3.35
	3	60.0	II	0.07	480,000/34,400	3.90/2.85

[a] $w_3 = 0.03$; $\Delta w_2 = 0.01$ (comp. 1); 0.05 (comp. 2); 0.09 (comp. 3).
$\Delta w_2 = w_2 - w_{2,cp}$ with $w_{2,cp}$ = weight fraction of the nonsolvent at the cloud point.

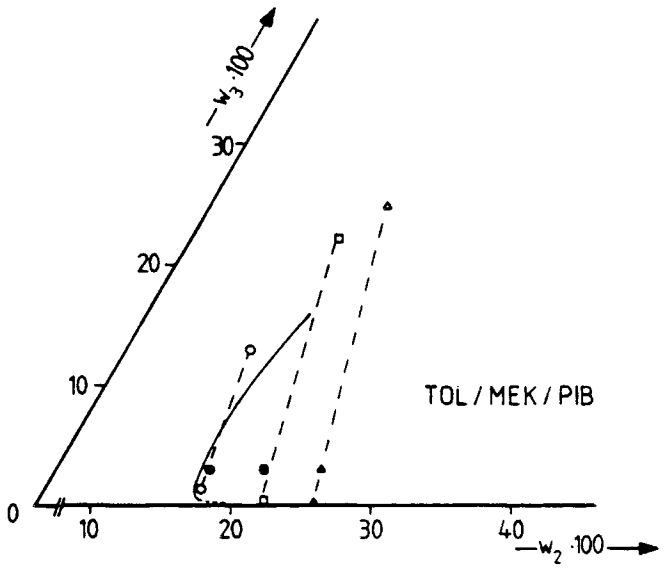

Fig. 4. Cloud point curve and some tie lines for the system toluene/methyl ethyl ketone/PIB I at 22°C.

concentration? To find the answer, the average molecular weights of the polymer contained in the sol and in the gel phase, respectively, are plotted in Figures 5(a) and 5(b) as a function of G for the different mixed solvents. Since the molecular weight distribution of the original product shows a pronounced high molecular weight tail, more details can be seen from the gel than from the sol branches. According to the information of Figure 5, the combinations TOL/MEK, DBE/MEK, and HEP/MEK appear promising whereas CH/AC and HEP/IPA can practically be ruled out. Table III gives a more quantitative comparison in terms of the differences in the molecular weights of gel and sol at $G = 0.5$.

In view of future applications of the CPF to other polymers, it was checked whether the components of the mixed solvents leading to the best fractionation (Table III) are thermodynamically the most similar ones, as postulated by theoretical considerations. For this comparison the solubility parameters of the components and a, the exponent of the Kuhn–Mark–Houwink equation, are collected in Table IV.

The solubility parameters of the nonsolvent components in combination with those of the polymer leads to the observed order of solvent power (cf.

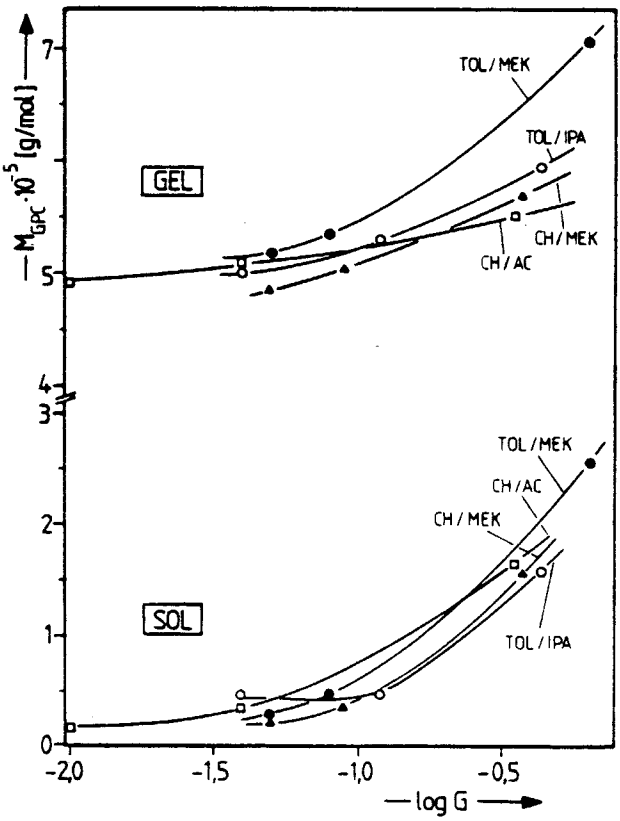

Fig. 5(a),(b). Dependence of the average molecular weight (as estimated from the GPC maxima) of the polymer contained in the coexisting sol and gel phase, respectively, on log G, where G is the mass of the polymer in the sol to that in the gel; G is varied isothermally (22°C) via the composition of the mixed solvent for solutions containing 3 wt % polymer.

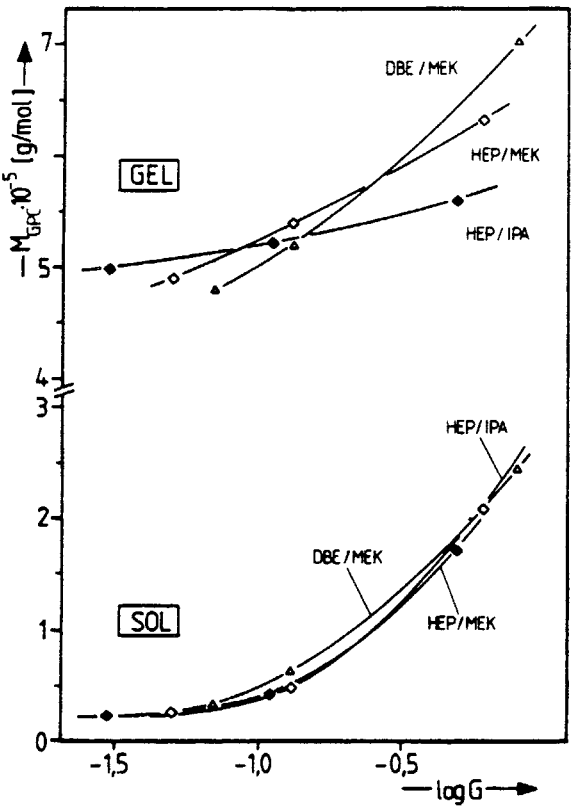

Fig. 5(b). (*Continued from the previous page.*)

TABLE III
Difference of the Molecular Weights of the Polymers Contained in the Coexisting Phases at $\dot{G} = 0.5$ for Various Mixed Solvents

Mixed solvent	$(\Delta M = M^{GL} - M^{SL})_{GPC}$
TOL/MEK	455,000
TOL/IPA	430,000
HEP/MEK	442,500
HEP/IPA	385,000
CH/MEK	392,500
CH/AC	360,000
DBE/MEK	455,000

Fig. 3); for the estimation of the solvent power of the solvent components, the a values are preferred since they stem from actual measurements with the binary system and do not contain theoretical assumptions.

The combination of a given solvent with any one of the different available nonsolvents will produce a system that is more apt for fractionation, the closer this nonsolvent is positioned to the solvent in Table IV; the same holds true for combinations of a, given nonsolvent with the different solvents. It can therefore be concluded that the search for thermodynamically similar components of the mixed solvent is indeed a proper guide to find the best system.

TABLE IV
Solubility Parameters and Kuhn–Mark–Houwink Exponents a

Component	δ (cal/cm^3)$^{0.5}$*	a_{25} (°C)
PIB	7.7–8.4[8]	—
CH	8.2[9]	0.76[11]
HEP	7.45[9]	0.70[11]
DBE	7.64[9]	—
TOL	8.9[9]	0.56[12]
MEK	9.0–9.3[10]	—
AC	9.4–10[9]	—
IPA	11.5[9]	—

*1 cal$^{1/2}$ cm$^{-3/2}$ = 2.045 × 10^{3}J$^{1/2}$ m$^{-3/2}$.

Further properties of the mixed solvent/polymer systems, in addition to the fractionation efficiency itself, have, however, to be considered. The most important ones are discussed in the following.

Influence of the Composition of the Mixed Solvent

Figures 6(a) and (b) show how G varies with the content of nonsolvent; in this graph w_2 is decreased by $w_{2,cp}$, the fraction of nonsolvent at the cloud point. In view of the CPF, the slope of these curves is of special interest, since it measures the sensitivity of G against fluctuations in the composition of the mixed solvent. TOL/IPA turns out to be the least and CH/AC the most sensitive combination; all other mixed solvents fall in between.

Influence of Temperature. The variation of T at constant composition of the mixed solvent is of similar practical importance as the isothermal variation of w_2. With the present equilibrium experiments (all performed at 22°C) the information can, however, only be gained in an indirect manner by measuring the distance of the cloud point temperature T_{cp} (cf. Table II) from this equilibrium temperature T_{eq} for the different solutions under investigation. The results are given in Figure 7. From this evaluation the correspondence of the variables temperature and composition of the mixed solvent can be read for each experiment. Systems which are more sensitive against changes in T than others manifest themselves by small slopes of the curves in Figure 7; conversely, these slopes become higher as the sensitivity with respect to the variation of w_2 gains importance.

The CPF demands a mixed solvent that is not too sensitive against either of the two variables in order to exclude problems due to inevitable fluctuations in these working parameters. On the other hand, the T influence should be high enough to allow a quick and effective change (e.g., a correction) of the operating conditions via T.

Ease of Phase Separation. In order to study this kinetic aspect under the most crucial conditions, solutions containing ca. 3 wt% of the polymer were titrated to constant turbidity (cf. determination of cloud points) at 22°C. It was then observed how quickly the droplets coalesce and how long it takes until two completely clear phases have formed. The results of these experiments are compiled in Table V. It turns out that the systems containing DBE separate particularly slowly. The combinations HEP/IPA, HEP/AC,

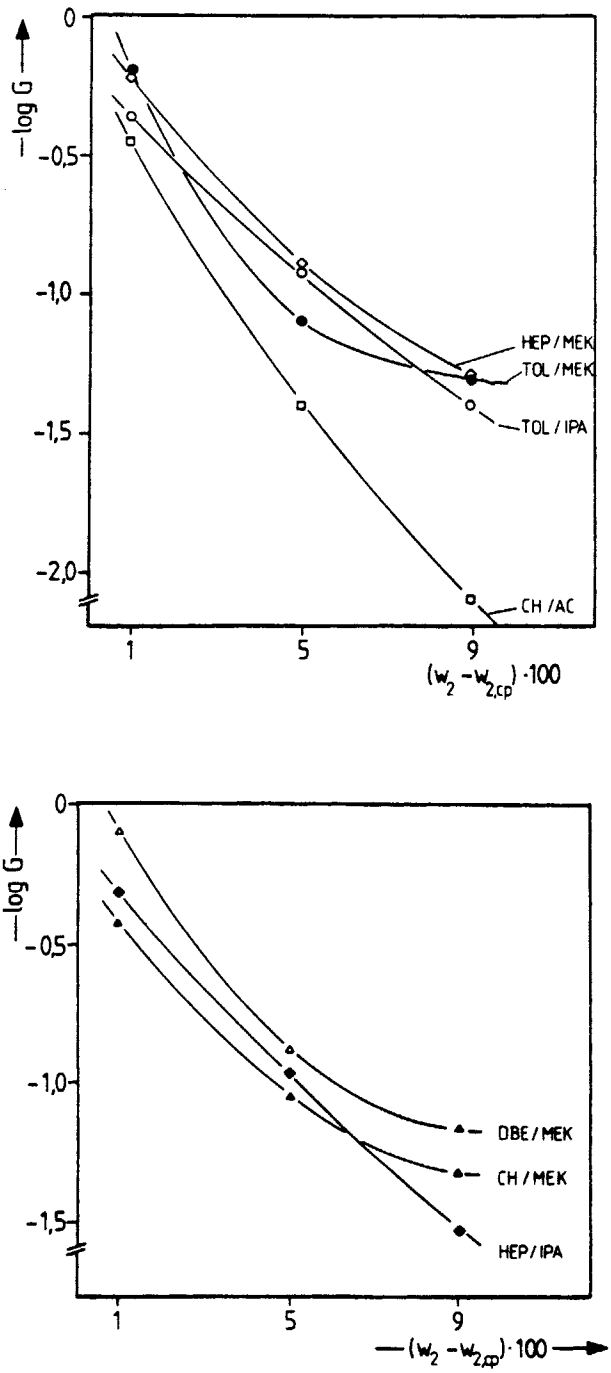

Fig. 6(a), (b). Influence of the surplus of the nonsolvent $w_2 - w_{2,cp}$ (actual weight fraction − weight fraction at the cloud point) on the mass ratio G of the polymer in the sol to that in the gel phase; the concentration of PIB I in the indicated mixed solvents (for abbrev. cf. Table I) was 3 wt %, $T = 22°C$.

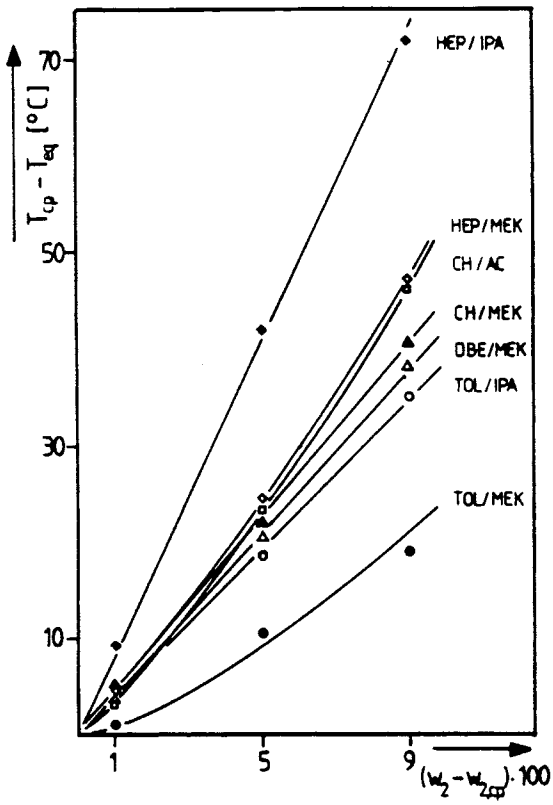

Fig. 7. Equivalence of the surplus of the nonsolvent $w_2 - w_{2,cp}$ (actual weight fraction − weight fraction at the cloud point) and $T_{cp} - T_{eq}$ (difference between cloud-point and equilibirium temperature); the concentration of PIB I in the indicated mixed solvents (for abbrev. cf. Table I) was 3 wt %, T_{eq} = 22°C.

TOL/AC, and TOL/MEK, on the other hand, form completely clear phases after only a few hours. At least three variables influence the rapidity of phase separation: Differences in the densities of the coexisting phases plus the interfacial tension between them and the viscosity of the continuous phase. According to the experimental observations, the first variable obviously plays only a minor role, since the TOL containing systems show similar densities,

TABLE V
Observations Concerning the Time Dependence of Phase Separation[a]

Solvents \ Nonsolvent	IPA	AC	MEK
TOL	ca. 12 h (q)	ca. 1 h (q)	ca. 1 h (q)
HEP	ca. 1 h (q)	ca. 1 h (q)	> 1 days (q)
CH	> 2 days (s)	ca. 12 h (m)	> 1 days (s)
DBE	> 2 days (s)	ca. 2 days (s)	> 2 days (s)

[a] In addition to the time required for the formation of completely clear coexisting phases, the rate of coalescence of the segregated droplets to continuous but still turbid phases is indicated in parentheses: q = quick (< 10 min), m = medium (10 min–1 h), s = slow (> 1 h).

but belong to the most rapidly separating ones. The viscosity of the continuous phase, on the other hand, gives a better correlation, i.e., low viscosities of the mixed solvents are associated with a rapid sedimentation of segregated droplets. Studies concerning the influence of the magnitude of interfacial tension on the kinetics of phase separation are planned.

First CPF Runs

The mixed solvent TOL/MEK was chosen for the following reasons: The best equilibrium fractionation efficiency is observed with the nonsolvent MEK in combination with either of the solvents TOL, DBE, and HEP, where TOL combines quick phase separation with comparatively low price and easy handling. The present CPF runs should yield first experience with PIB and a number of good fractions of high molecular weight; systematic studies concerning the best operating conditions of the CPF are reported in part II of this series, together with a discussion of additional aspects to be considered with this nonequilibrium method.

Figure 8 shows by means of the corresponding phase diagram the composition of FD and EA chosen for the first fractionation step; the working point (composition of entire content of the counter-current column) is also indicated. Under the present conditions, comparatively large flakes, impeding the transport through the sieve bottoms, are formed as the FD flows down the column instead of the tiny droplets resulting in the case of PVC[2]; the most probable reason for this behavior lies in the very high molecular weight material contained in this phase. Nevertheless, it was possible to operate the CPF under the conditions shown in Table VI for over ca. 50 h, so that more than 2 kg of the original PIB could be fractionated. Approximately 70% of the

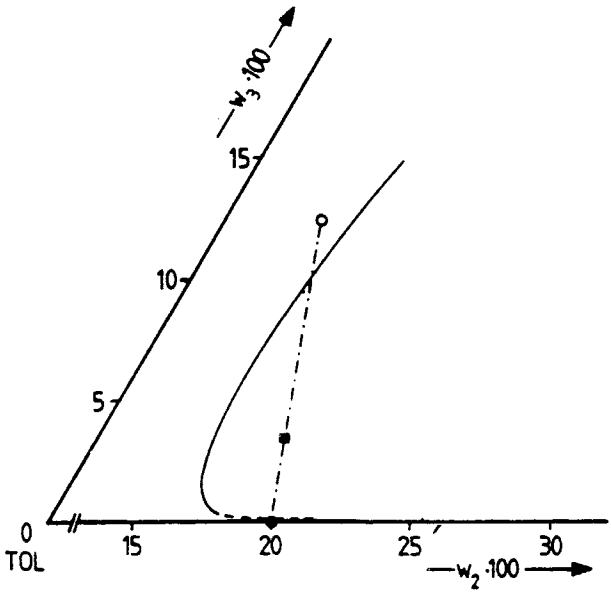

Fig. 8. Phase diagram of the system toluene/methyl ethyl ketone/PIB I at 22°C, showing the composition of the phases for the first CPF-step: (○) feed; (●) extracting agent; (■) working point.

TABLE VI
Working Parameters (a) and Experimental Results (b) of the CPF

(a) Working parameters

Step	w_2^{FD}	w_3^{FD}	w_2^{EA}	$\dot{V}^{FD}/\dot{V}^{EA}$ (cm³/min)	$\dot{m}_3^{FD}$ (g/min)	A[a]	[a]	T (°C)	M^{FD}[b] g/mol	U^{FD}[c]	Remarks
I	0.155	0.125	0.20	5.0/18.0	0.54	18	3.5	22	420,000[a]	2.3	FDI → PIB I
II	0.149	0.142	0.1975	5.0/22.5	0.61	18	3.0	22	600,000	1.5	FDII → Gel I
III	0.180	0.076	0.193	4.0/18.0	0.26	15	2.0	25	700,000	1.1	FDIII → Gel II
IV	0.166	0.069	0.189	3.5/19.0	0.21	15	2.0	25	950,000	0.6	FDIV → Gel III

(b) Experimental Results

Step	$\dot{V}^{GL}$ (cm³/min)	$\dot{V}^{SL}$ (cm³/min)	w_3^{GL}	w_3^{SL}	$\dot{m}_3^{GL}$ (g/min)	$\dot{m}_3^{SL}$ (g/min)	$\dot{G}$	M_w^{GL}[b] (g mol⁻¹)	U_{GL}[c]	M_w^{SL}[b] (g mol⁻¹)	U^{GL}[c]
I	3.10	20.0	0.148	0.0070	0.38	0.15	0.39	600,000*	1.5	—	—
II	3.80	23.7	0.140	0.0060	0.45	0.12	0.27	700,000	1.1	350,000	1.0
III	1.73	20.3	0.102	0.0056	0.15	0.10	0.67	950,000	0.6	420,000	0.57
IV	1.79	20.8	0.0978	0.0031	0.15	0.055	0.37	1,100,000*	0.3	610,000*	0.30

[a] Scale readings on the CPF apparatus used; cf. Part II.
[b] In all cases M_w was determined by GPC; additional light scattering measurements are indicated by an asterisk (in this case the average value is given).
[c] U calculated from M_w and M_n of GPC measurements.

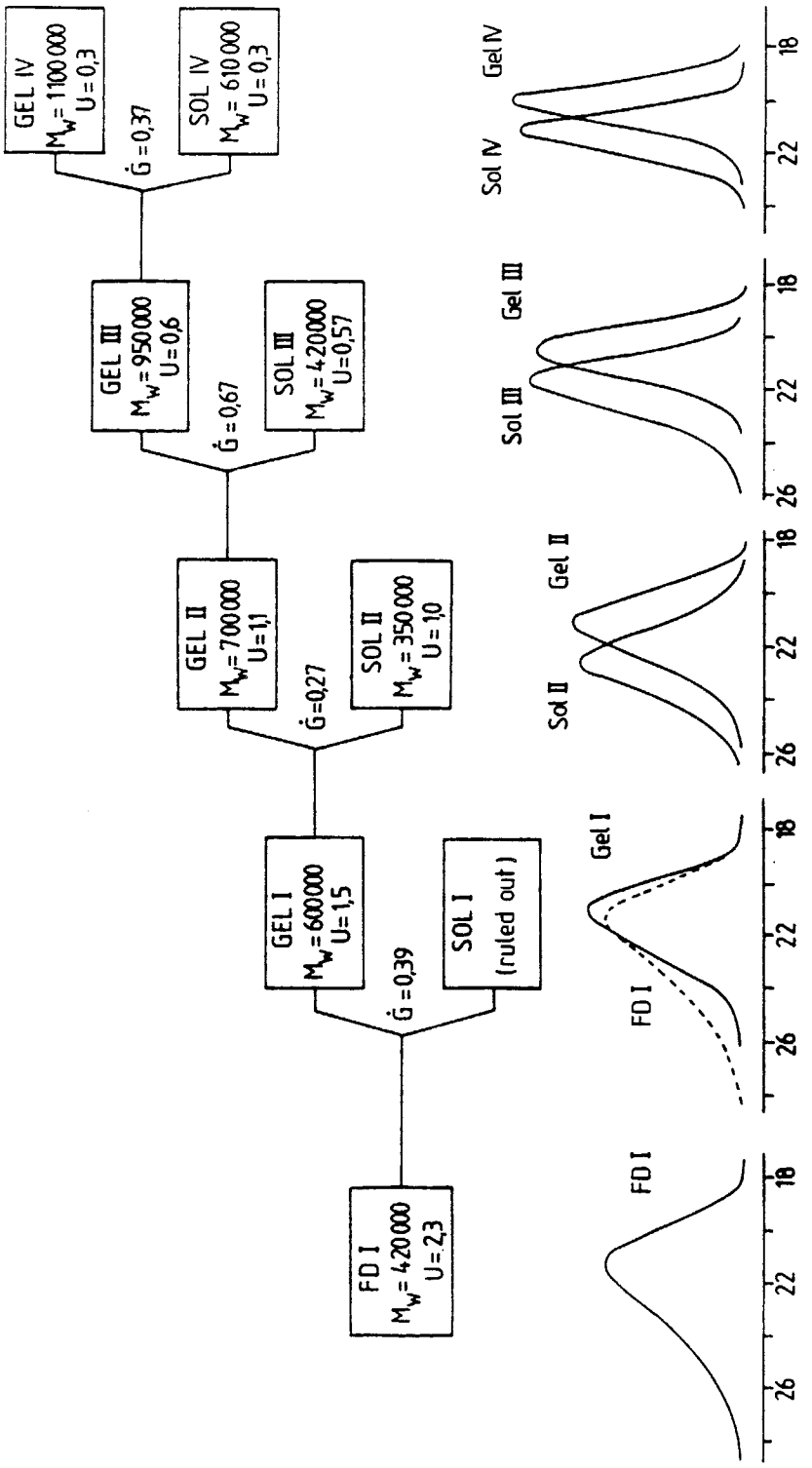

Fig. 9. Scheme of a fractionation procedure consisting of four CPF steps performed with PIB I using the mixed solvent toluene/methyl ethyl ketone; $\dot{G}$ = weight ratio of the polymer delivered per unit time in the sol phase to that delivered in the gel phase, M_w = weight average molecular weight, U = molecular nonuniformity $(M_w/M_w) - 1$, M_n = number average molecular weight). The lower part of the diagram shows the normalized GPC curves for the original polymer and for the different fractions.

starting material was contained in the GL phase (GL I: M_w = 600,000; U = 1.5) and refractionated in the second step (cf. Table VI) to yield SL II and GL II. After that, again only the polymer contained in the gel was refractionated. The details of the entire procedure, consisting of 4 CPF steps and leading to ca. 700 g of good fractions, can be seen from Figure 9 and Table VI.

In the course of the above experiments, several new problems, obviously characteristic for very high molecular weight material, had to be overcome. In particular, it turned out that the concentration of the polymer in the FD has to be lowered considerably in conjunction with a reduction of its flow rate, so that the average polymer concentration in the column becomes sufficiently low. Furthermore, the subdivision of the polymer contained in the FD into the SL and GL (measured by $\dot{G}$) proves extremely sensitive against even minute changes in the operating conditions.

In conclusion, it can be stated that the CPF is successfully applicable even to quite high molecular weight material; the problems, however, increase (like with all other methods based on solubility) almost exponentially as the weight average degree of polymerization passes (at constant molecular nonuniformity) beyond a certain critical limit. According to the present data, this value is on the order of 15,000 for $U < 0.5$.

The present work was sponsored within the scope of the "industrielle Gemeinschaftsforschung" by the "Bundesminister für Wirtschaft" of the FRG. This support is gratefully acknowledged.

The authors thank the BASF, Ludwigshafen for providing the starting PIB products.

References

1. Ger. Pat. Angem., P 32 42 1033 (1982), invs., B. A. Wolf, H. Geerissen, J. Roos, and P. Amareshwar.
2. H. Geerissen, J. Roos, and B. A. Wolf, *Makromol. Chem.*, **186**, 753 (1985), Part 1.
3. J. Brandrup and E. H. Immergut, *Polymer Handbook*, 2nd ed., Wiley-Interscience, New York, 1975 p. IV-273.
4. K. C. Berger and G. V. Schulz, *Makromol. Chem.*, **136**, 221 (1970).
5. G. Greschner, Private communication.
6. C. A. Baker and R. J. P. Williams, *J. Chem. Soc. (London)*, 2352 (1956).
7. B. A. Wolf, *Adv. Polym. Sci.*, **10**, 160 (1972).
8. H. Gnamm and O. Fuchs, *Lösungsmittel und Weichmachungsmittel*, WVG, Stuttgart, 1980, Bd. 1, pp. 594ff.
9. H. Gnamm and O. Fuchs, Ref. 8, pp. 86ff.
10. J. Bradrup and E. H. Immergut, Ref. 3, p. IV-337.
11. H. Gnamm and O. Fuchs, Ref. 8, p. 786.
12. J. Brandrup and E. H. Immergut, Ref. 3, p. IV-8.

Received July 30, 1986
Accepted November 7, 1986